Research on Pressure Loss and Filling Ability of Semi-Solid Rheological Behavior in Squeeze Casting

Ying Wang
Beijing Institute of Technology
Xiaohui Ao (xhao@bit.edu.cn)
Beijing Institute of Technology

Research Article

Keywords: Pressure loss, Filling ability, Semi-solid, Rheological behavior, Squeeze casting

Posted Date: October 11th, 2021

DOI: https://doi.org/10.21203/rs.3.rs-893427/v1

Research on Pressure Loss and Filling Ability of Semi-solid Rheological Behavior in Squeeze Casting

Ying Wang[2]·Xiaohui Ao[1]

1. School of Mechanical Engineering, Beijing Institute of Technology, Beijing 100081, China;
2. School of Mechatronics and Vehicle Engineering, Zhengzhou University of Technology, Zhengzhou 450044, China
Corresponding author: Xiaohui Ao xhao@bit.edu.cn;

Abstract

The filling ability of alloy fluid under pressure is of great significance to improve the dimensional integrity and mechanical properties of thin-walled and slender rods formed by squeeze casting. Insight into the rheological behavior of squeeze casting is beneficial to improve the formability of complex structural parts by optimizing the squeeze casting process. In this work, the Archimedes spiral sample prepared by indirect squeeze casting was applied to investigate the variation of filling length with squeeze pressure and filling speed during the rheological process in squeeze casting. According to the temperature distribution characteristic during the alloy melt filling process, the alloy fluid state was discussed and the spiral filling was confirmed as a semi-solid rheological behavior. The calculation models of pressure loss and filling length were established respectively based on steady-state rheological behavior. Pressure loss is mainly affected by the melt viscosity which is determined by temperature distribution and filling speed of alloy melt in the channel. According to the agreement between the theoretical calculations and the experimental results, the pressure loss and filling length models have been confirmed to be used to quantitatively characterize the filling ability of the aluminum alloy melt in the squeeze casting process.

Keywords： Pressure loss; Filling ability; Semi-solid; Rheological behavior; Squeeze casting

1. Introduction

The filling ability of alloy melt has a very important influence on the integrity and the surface roughness of the castings especially thin-walled and thin-rod parts with complex structures[1-3]. Due to applying the pressure to the melt poured into the mold cavity has significantly improved the filling ability of castings, the squeeze casting has been widely used in the solidification manufacturing [4-5]. However, the alloy melt flowing in the channel with a small radius has a

large cooling rate and easily cause a large viscosity, so the mechanism of this rheo-filling process is very complicated, which severely restricts the formation of high-performance and ultra-thin structural castings by squeeze casting[6-7]. Although increasing the pressure of squeeze casting can continuously improve the filling ability, it would significantly reduce the life of the mold and increase the cost of the pressure equipment. Therefore, a more effective method to improve the melt filling ability is of great significance to squeeze casting thin-walled and thin-rod parts.

In order to quantitatively improve the filling ability of squeeze casting and predict the filling length by optimizing process parameters, many experimental and theoretical studies have been made in squeeze rheological casting[8-10]. In addition to increasing the pressure and optimizing the mold structure, a variety of process measures have been adopted to improve the filling ability. The influences of melt temperature, applied pressure and filling speed on the rheo-filling ability of semi-solid A356 alloys were studied and the optimal ranges of these parameters were determined separately by Bai et al.[11]. Zhang et al.[12] developed a theoretical evaluating model to predict the maximum filling length based on the flowing theory of the incompressible viscous fluid and believed that the filling pressure and filling speed are prominent influencing factors on the mold-filling ability of alloy melt. Obviously, increasing the pouring temperature is also benefit on the filling ability of alloy melt, but it should not be too high, otherwise it would easily cause the defects of entrainment in the rheological squeeze casting[13-14]. Many studies have also shown that chemical composition and fine-grained structure were beneficial to the filling ability of aluminum alloys[15-17]. However, the method of calculating filling ability and pressure loss of semi-solid rheological behavior in squeeze casting is still unclear and cannot provide guidance for squeeze casting of thin-walled parts.

In fact, the melt viscosity affected by the shear rate and temperature is the essential factor that resists the melt filling ability[18]. Li et al. [19] found that the apparent viscosity of semi-solid 7075 aluminum alloy decreases with an increase in shearing rate and believed there is a shearing thinning phenomenon, which could be attributed to less liquid being entrapped in the solid particles. Blanco et al. [20] studied the rheological behavior of the semi-solid Al-5Cu melt using a high temperature Searle rheometer and the results show that the higher the shear rate, the lower the apparent viscosity of the semi-solid Al-5Cu melt. Many researchers agree that the relationship between apparent viscosity and shear rate conforms to the power law[21-23]. However, for the

filling of alloy melts, it is not possible to directly calculate the apparent viscosity with an unmeasurable shear rate, which brings a great challenge to the prediction of filling length. In addition, the variation of pressure loss during alloy melt filling process is unclear, which makes it difficult to quantitatively optimize process parameters according to the requirements for the integrity and mechanical properties of castings. Therefore, the mechanism of pressure loss and filling ability of semi-solid rheological behavior in squeeze casting needs to be further revealed.

In this paper, the Archimedes spiral experiment of A356 aluminum alloy in squeeze casting with different pressures and filling speeds was carried out. The temperature distribution of A356 alloy melt along the spiral channel in the filling process was calculated and the fluid state was analyzed. The calculation models of pressure loss and filling length were established respectively based on steady-state rheological behavior and the influence factors on them were quantitatively discussed. The rheological mechanism of squeeze casting was further revealed, which have provided an important basis for forming high-quality castings and optimizing process parameters.

2. Experimental procedure

In order to insight into the mechanism of squeeze pressure loss during the semi-solid alloy rheological process, a spiral squeeze casting experiment was conducted using a self-designed spiral mold as shown in Fig. 1. The spiral mold is mainly divided into four parts, namely upper die, lower die, punch and chamber. There is an Archimedes spiral channel with a length of 1350 mm and a radius of 4 mm in the upper die. The lower die is a cylindrical chamber, which connects with the Archimedes spiral cavity by the channel on the side wall. The commercial A356 aluminum alloy is used and its chemical composition is shown in Table 1.

Table 1 Chemical compositions of A356 alloy (wt.%)

Si	Mg	Fe	Cu	Ti	Sr	Zn	Ni	Al
7.153	0.394	0.127	0.085	0.007	0.007	0.008	0.004	Bal.

The A356 alloy was melted in an electrical furnace of 5 kW, and the temperature was measured by TES-1310 type contact thermometric instruments and K-type thermocouples. When the melt temperature reached 990±5 K, CCl4 (2 wt.%) was added to refine the alloy melt. Ten minutes later, it was slagged off. The alloy liquid was allowed to stand, and when the temperature was adjusted to 990 K, it was directly poured into the lower die with a preheated temperature of 440 K. Then the punch moved down driven by the filling cylinder to squeeze the alloy melt back

into the upper cavity. The punch was reset after the holding time of 20 s. The pressure was removed from the movable beam, which drove the upper die to reset. Lastly, the sample was ejected out of the mold by ejectors. The spiral specimens were prepared under the squeeze pressure of 20, 50 and 80 MPa and the filling speed of 0.01, 0.02, and 0.05 m/s, respectively.

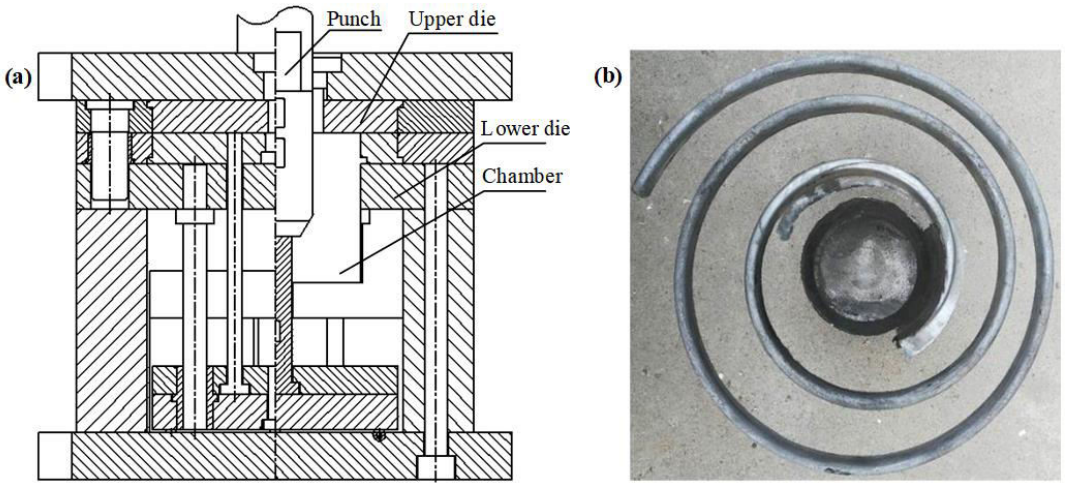

Fig. 1 (a) Self-designed spiral mold structure diagram and (b) spiral specimen.

3. Results

Variation of filling length with squeeze pressure and filling speed is presented in Fig. 2. It can be seen that both the squeeze pressure and the filling speed can be considered to have a linear influence on the filling length. The influence of squeeze pressure on the filling length is not obvious with a small filling speed, and as the filling speed increases, the promotion influence of the squeeze pressure on the filling length becomes more significant. Compared with the squeeze pressure, the filling speed has a more obvious influence on the filling length shown as in Fig2(b). In fact, the volume fraction and morphology of the primary phase are important factors affecting the apparent viscosity of the semi-solid melt. When the filling speed is higher, the semi-solid A356 melt has a smaller volume fraction. This is because the higher shear rate can break large-size dendrites into fine equiaxed crystals[24], which is beneficial to reduce the apparent viscosity of the melt and improve the filling ability. Fig. 3 shows the microstructure morphology at the filling speed of 0.01, 0.02 and 0.05 m/s, respectively, with the squeeze pressure of 50 MPa. With the increase of the filling speed, the crystal grains changed from dendritic to equiaxed, indicating that the high shear rate has a good shearing effect on the primary dendrites.

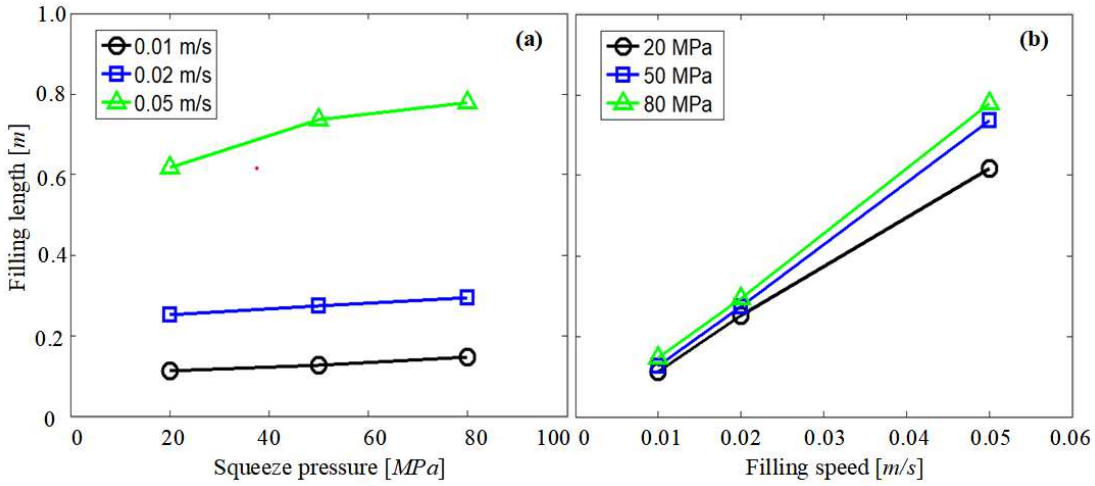

Fig. 2 Variation of filling length with (a) squeeze pressure and (b) filling speed.

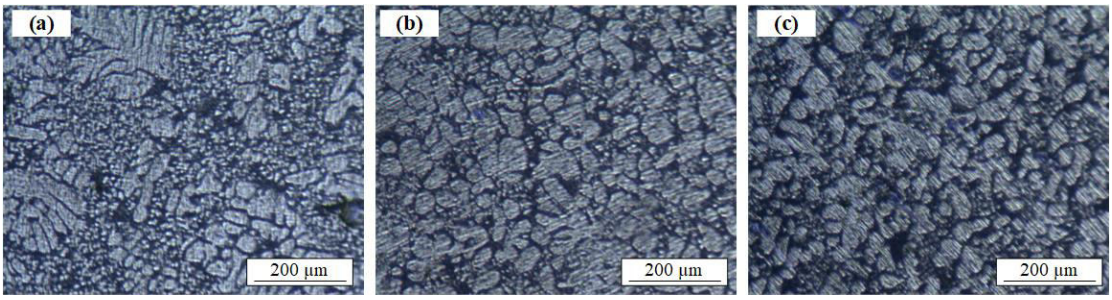

Fig. 3 Microstructure morphology at the filling speed of (a) 0.01 m/s; (2) 0.02 m/s; and (3) 0.05 m/s, respectively.

4. Discussion

The semi-solid rheo-filling process of spiral experiment is usually divided into two stages: increasing pressure and maintaining pressure. In the stage of increasing pressure, the filling speed is constant and equal to the set value v_{set}, and the squeeze pressure gradually increases to the maximum value, i.e., the set squeeze pressure P_{set}. Because the heterogeneous nucleation undercooling is small and the melt temperature near the channel wall is lower than that in the center of the channel, the solid phase is first precipitated on the inner wall of the channel. Then, under the scouring action of the subsequent overheated melt, the solidified solid phase on the channel wall is partial remelted and mixed into the alloy melt to form a semi-solid slurry. The fluid state is also transformed from Newtonian fluid to non-Newtonian fluid. Therefore, the spiral filling process can be regarded as a semi-solid solidification behavior. When the squeeze pressure reaches the set value P_{set}, the stage of maintaining pressure begins. Due to the decrease of melt temperature and the continuous increase of filling length, the viscous resistance of the alloy melt is greater than the applied squeeze pressure P_{set}, so the filling speed v starts to decrease until the melt stops filling.

According to the melt state and filling characteristics, the pressure loss P_{loss} can be divided into three parts and the classification method is shown in Fig. 4. Firstly, in the stage of increasing pressure when the melt is filled at a constant speed v_{set}, the pressure loss consists of pressure loss P_1 caused by liquid melt length L_1 and pressure loss P_2 caused by semi-solid melt length L_2. While the pressure loss P_3 is caused by semi-solid melt length L_3 in the stage of maintaining pressure. In the stage of increasing pressure, there is a relationship between the applied squeeze pressure P_a and the pressure loss caused by the filling melt: $P_a=P_1+P_2-P_0$, P_0 is the atmospheric pressure. Compared with the squeeze pressure of squeeze casting, the atmospheric pressure can be ignored, and thus it can be considered that the pressure loss during the rheo-filling process is equal to the applied squeeze pressure. While in the stage of maintaining pressure, the relationship between the maximum appied squeeze pressure P_{set} and the pressure loss caused by the filling melt P_{loss} is: $P_{set}<P_{loss}$.

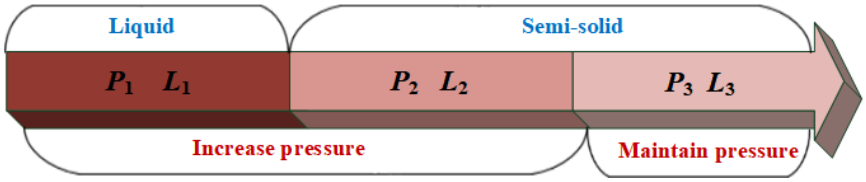

Fig.4 Classification method of pressure loss according to the melt state and filling characteristics.

4.1 Temperature characteristic

During the alloy melt filling process, the melt temperature characteristic is one of the main factors affecting the filling resistance, which ultimately determines the interaction relationship between the filling length and the squeeze pressure. When the alloy melt flows into the spiral channel, the heat will be transferred to the mold through heat conduction. The melt temperature distribution during the filling process can be calculated based on the following assumptions: (i) the temperature of the mold keep constant; (ii) the heat convection and radiation are neglected; (iii) the heat convection of alloy melt along the spiral channel is ignored.

According to the heat balance principle and $dx=vdt$, the heat balance relationship at x from the beginning of the spiral channel can be expressed as:

$$\frac{h(T-T_0)}{v}dSdx=-\rho CdVdT\,, \tag{1}$$

where $h=0.0011P^3-0.112P^2+6.605P+2924.57$ the heat transfer coefficient between melt and the mold[25], T the melt temperature at x, T_0 the mold temperature, dS and dV are the unit heat

conduction area and unit melt volume at x respectively and the relationship between them is $dV/dS = R/2$, R the spiral channel radius, ρ the density of alloy melt, C the equivalent specific heat capacity, for the melt and semi-solid melt which can be respectively expressed as:

$$C = C_0 \text{, for melt} \tag{2}$$

$$C = C_0 - \frac{df_s(T)}{dT}\Delta H \text{ , for semi-solid melt} \tag{3}$$

where C_0 the specific heat capacity, ΔH the enthalpy change of alloy melt, f_s the solid fraction and its variation with temperature obtained through DSC analysis can be expressed as[26]:

$$f_s(T) = 94.63\left[\frac{0.00478}{1+10^{-0.397(832.44-T)}} + \frac{0.99522}{1+10^{-0.0184(1004.84-T)}}\right] - 93.61, \tag{4}$$

Integrating Eq. (1) with a constant filling speed, the relationship between the melt temperature and the filling length can be expressed as:

$$T = (T_c - T_0)\exp\left(-\frac{2hL}{v_{\text{set}}R\rho C_0}\right) + T_0 - \Delta f_s(T)\Delta H/C_0 , \tag{5}$$

where T_c the pouring temperature, Δf_s the solid fraction difference.

In order to understand the variation of the melt temperature along the spiral channel at a constant filling speed and whether the filling melt is in a liquid or semi-solid state, the temperature distribution and filling length of the alloy melt were calculated and analyzed. Thermophysical properties of A356 alloy used was shown in Table 2. When the melt temperature drops to the eutectic temperature, the solid fraction increases rapidly, so it is reasonable to assume that the melt has to stop filling at this temperature point.

Table 2. Thermophysical properties of A356 alloy[27].

Property and symbol	Value
Spiral channel radius R (m)	0.005
Initial mold temperature T_0 (K)	443
Specific heat capacity C_0 ($J\cdot K^{-1}\cdot kg^{-1}$)	963
Enthalpy change ΔH ($J\cdot kg^{-1}$)	398000
Density ρ ($kg\cdot m^3$)	2650
Liquidus temperature T_l (K)	888

Fig.5 shows the relationship between the melt temperature along the spiral channel and the

filling length at different pouring temperatures. It can be seen that when the alloy melt flows into the spiral channel, its temperature quickly drops to the liquidus with a short filling length, which indicates that the pouring temperature has little influence on the filling length. Then due to the release of enthalpy during the solidification process, the melt temperature drops slowly and the filling length increases linearly and significantly with melt temperature. With the decrease of the melt temperature, the solid fraction is increased to improve the filling resistance. When the temperature of alloy melt reaches the eutectic temperature, the rapid solidification of alloy melt leads to a large filling resistance to prevent continued filling. Fig.5(b) shows the variation of filling length of the spiral channel at different pouring temperatures. When the pouring temperature is lower than the alloy liquidus temperature, the pouring temperature has a greater influence on the filling length of the spiral channel. However, when the pouring temperature is higher than the alloy liquidus temperature, as the pouring temperature increases, the filling length increases slowly. This phenomena indicate that the alloy liquid in spiral channel is mainly the semi-solid melt.

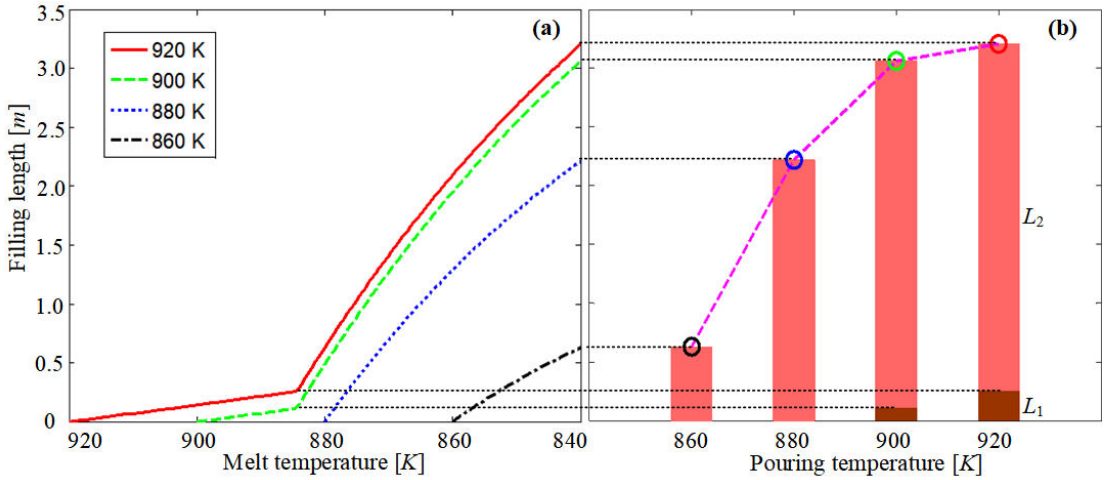

Fig.5 Relationship between the melt temperature along the spiral channel and the filling length at different pouring temperatures.

4.2 Apparent viscosity characteristic

It is generally believed that the semi-solid melt is a non-Newtonian fluid, and its apparent viscosity is not only related to the melt temperature, but also related to the shear rate. When the melt temperature decreases to below the liquidus, the power law model has been formulated to describe the apparent viscosity model for semi-solid A356 alloy melt[28]:

$$\eta(T,\gamma) = K\gamma^{n-1}, \tag{6}$$

$$\gamma = \frac{6n+2}{2n+1}\frac{v}{R}, \tag{7}$$

where, the coefficient n and K were obtained by Ma et al.[29]:

$$n = -0.00866(T-273)+5.225. \tag{8}$$

$$K = 10^{\frac{3.434}{1+\exp[(T-868.066)/2.899]}+3.594} \tag{9}$$

So Eq(6) can be transformed into:

$$\eta(T,v) = \left(\frac{3n+1}{2n+1}\frac{v}{R}\right)^{[n-1.4]} 10^{(-0.094T+60.263)}. \tag{10}$$

In fact, the solid fraction and morphology of primary α-Al are the direct factors that affect the apparent viscosity of the semi-solid melt of A356 alloy. Fig.6 shows the variation of apparent viscosity and solid fraction with decreasing melt temperature at different filling speeds. As the temperature decreases, the precipitation of primary α-Al increases, which reduces the fluidity of the alloy melt. In particular, when the melt temperature is reduced to the eutectic temperature, the solid phase fraction increases rapidly, and the apparent viscosity of alloy melt should also increase rapidly. However, due to the difficulty of experimental measurement, it is assumed that the apparent viscosity at the eutectic temperature is so large that the alloy melt can no longer flow. In addition, it can be seen that increasing the filling speed is beneficial to reducing the apparent viscosity of the alloy melt and improving the filling ability of the alloy melt.

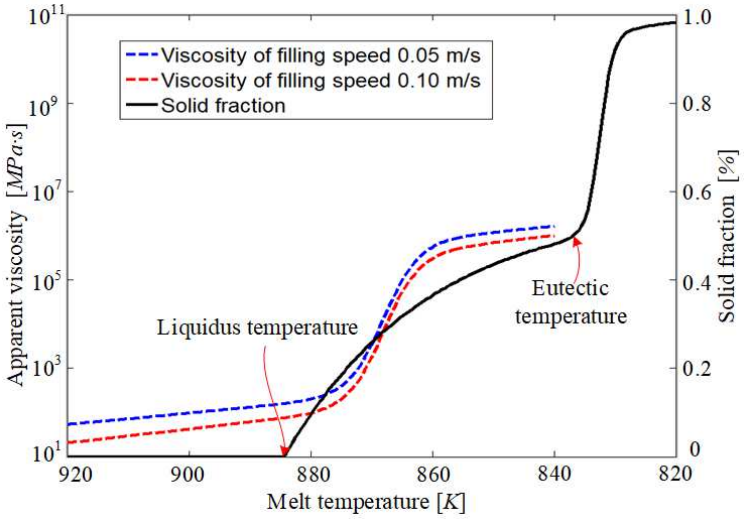

Fig.6 Variation of apparent viscosity and solid fraction with decreasing melt temperature at different filling speeds.

4.3 Pressure loss and filling length

According to Poiseuille's law, the pressure loss P_{loss} with the filling length of the alloy melt L

can be calculated as:

$$P_{\text{loss}} = 8\eta v L / R^2 \ , \tag{11}$$

where η the melt viscosity, v the filling speed, R the channel radius. Because the viscosity and flow speed of alloy melt at different temperatures and locations are different, the calculation of pressure loss is transformed into:

$$\int_0^{P_{\text{loss}}} dP = \int_0^L 8\eta v dx \Big/ R^2 \ . \tag{12}$$

When the melt temperature is greater than the liquidus temperature, it can be considered as a Newtonian fluid, and the viscosity is only related to the melt temperature. Therefore, combined Eq. (5) and Eq. (12), the filling length L_1 and pressure loss P_1 are calculated as:

$$L_1 = -\frac{v_{\text{set}} R\rho C_0}{2\text{h}} \ln \frac{T - T_0}{T_c - T_0}, \qquad T_l \le T < T_c \,, \tag{13}$$

$$P_1 = -\frac{4\rho C_0 v_{\text{set}}^2}{hR} \int_{T_c}^{T} \frac{\left(T_{\text{c}} - T_0\right)}{\left(T - T_0\right)} \eta(T) dT \,, \qquad T_l \le T < T_c \,. \tag{14}$$

Combined Eq. (1), Eq. (3) and Eq. (12), the filling length L_2 and pressure loss P_2 can be expressed respectively as:

$$L_2 = -\frac{vR\rho C_0}{2h} \ln \frac{T - T_0 + \Delta f_s(T)\Delta H / C_0}{T_l - T_0} \,, \qquad T_w \le T < T_l \tag{15}$$

$$P_2 = -\frac{4\rho v_{\text{set}}^2}{hR} \int_{T_l}^{T} \frac{T_l - T_0}{\left(T - T_0\right)} \eta\left(T, v_{\text{set}}\right) \left(C_0 - \frac{df_s(T)}{dT} \Delta H \right) dT \,, \qquad T_w \le T < T_l \,. \tag{16}$$

where γ the shear rate, where T_w is the temperature of the filling fluid's "head" when the applied squeeze pressure reaches the maximum P_{set}, i.e. P_{a}=P_{set}=P_1+P_2. There is also a relationship of $T_w \ge T_e$, T_e is the eutectic temperature of A356. If $T_w = T_e$, P_3=0 and the filling behavior stops.

When the squeeze pressure increases to the set maximum P_{set} and $T_w > T_e$, the squeeze pressure remains constant. As the filling length increases and the melt temperature decreases continuously, the filling speed is decreased caused by the pressure loss larger than the squeeze pressure and could be calculated as:

$$v = v_{\text{set}} - \int_0^{t_3} \frac{P_{\text{loss}} - P_{\text{set}}}{\rho L} dt \ , \tag{17}$$

Since (P_{loss}-P_{set})/ρL is much greater than v_{set}, the filling time at this stage is extremely short,

and thus the filling length $L_3 \approx 0$, $P_3 \approx 0$.

Therefore the variation of pressure loss with the decreasing melt temperature and along the filling length at different filling speeds can be calculated by Eq. (13)- (17) and shown as in Fig. 7. As the melt temperature decreases, the pressure loss increases rapidly, and when the melt temperature drops to 860 K, the actual squeeze pressure of more than 100 MPa is required to drive the further filling, which indicates that the filling has stopped when the melt temperature has not dropped to the eutectic temperature. The greater the filling speed, the greater the pressure loss, so the alloy melt with a larger filling speed will stop filling at a higher temperature. This is because the alloy melt with a larger filling speed can be filled for a longer distance at a higher temperature and the longer distance lead to a larger pressure loss.

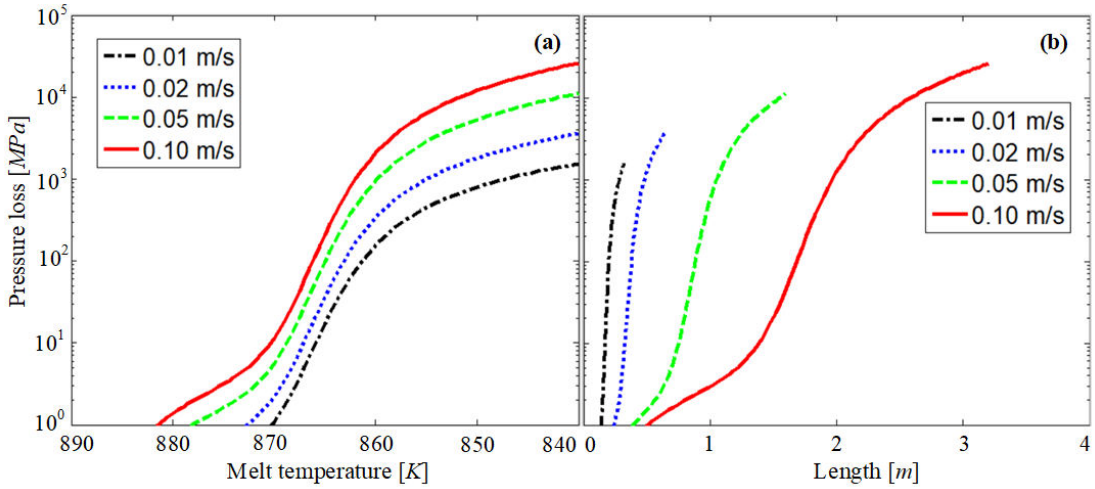

Fig. 7 Variation of pressure loss (a) with the decreasing melt temperature and (b) along the filling length at different filling speeds.

4.4 Verification

The comparison of filling lengths between theoretical calculation and experimental measurement of the spiral squeeze casting is shown in Fig. 8. It can be seen that the experimental filling lengths are basically in agreement with the theoretical calculations, but they are all less than the theoretical calculations, which is caused by ignoring the partial pressure loss of the spiral in the theoretical calculation. The greater the squeeze pressure, the more accurate the prediction of filling length. However, from the experimental results in Fig. 2 and theoretical calculation in Fig.7, it is not effective to increase the filling length by increasing the squeeze pressure, especially with a larger filling speed. While many studies have confirmed that increasing the squeeze pressure can effectively refine grains and improve mechanical properties[30-33].

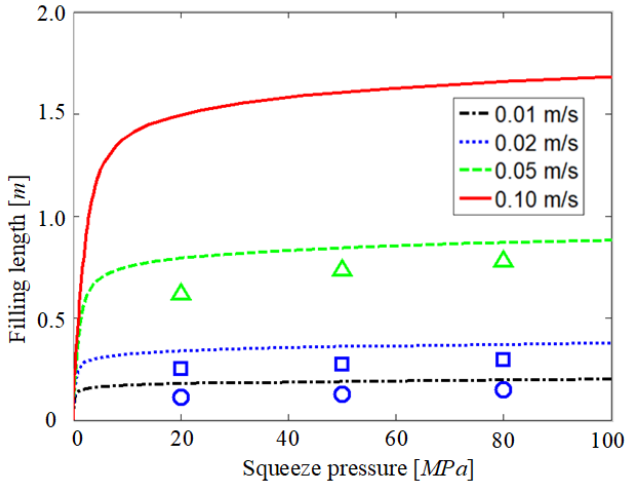

Fig. 8. Comparison of filling lengths between theoretical calculation and experimental measurement of the spiral squeeze casting

5. Conclusion

In this study, the influence of squeeze pressure and filling speed on filling length has studied by the spiral squeeze casting process and both the squeeze pressure and the filling speed can be considered to have a linear influence on the filling length. With fully considering the temperature and apparent viscosity characteristics of the semi-solid melt during the filling process, the prediction models of filling length and pressure loss are established separately, and the prediction results are in agreement with the experimental measurement. Increasing the filling speed is beneficial to the significant improvement of the filling ability, while the pouring temperature and the squeeze pressure have little influence on the filling length. The filling behavior of squeeze casting mainly occurs in the stage of increasing pressure, and the filling ability in the stage of maintaining pressure is very small. Therefore, it can be concluded that the dimensional integrity of the component is mainly determined by the filling speed and the mechanical properties are mainly determined by the squeeze pressure.

Author contribution Xiaohui Ao: Write original manuscript, Revise the paper, data processing and verify the results; Ying Wang: Experiment, data collection. All authors of this paper have read and approved the final versionsubmitted.

Funding This work was supported by the National Natural Science Foundation of China (Nos. 51905038, 51935003), Beijing Natural Science Foundation (No. 3204054), the National Key Research and Development Program of China (No. 2018YFB1105304), and the Youth Academic Launch Program of Beijing Institute of Technology.

Data availability The data in this paper are all obtained from experiments. All data generated during this study are included in this manuscript.

Declarations

Ethical approval My research does not involve ethical issues.

Consent to participate All authors have agreed to authorship, read and approved the manuscript, and given consent for submission and subsequent publication of the manuscript. The authors guarantee that the contribution to the work has not been previously published elsewhere.

Consent to publish All the authors agreed to publish this paper.

Competing interests The authors declare that they have no competing interests.

References

1. Dao V, Zhao S, Lin W, Zhang C (2012) Effect of process parameters on microstructure and mechanical properties in AlSi9Mg connecting-rod fabricated by semi-solid squeeze casting. Mater Sci Eng A 558:95-102.
2. Wang Y, Zhao S, Guo Y, Yang J (2020) Effects of process parameters on semi-solid squeeze casting performance of aluminum alloy scrolls for scroll compressors. China Foundry 17(5): 347-356.
3. Qi M, Kang Y, Xu Y, Wulabieke Z, Li J (2020) A novel rheological high pressure die-casting process for preparing large thin-walled Al-Si-Fe-Mg-Sr alloy with high heat conductivity, high plasticity and medium strength. Mater Sci Eng A 776:139040.
4. Jiang W, Zhu J, Li G, Guana F, Yu Y, Fan Z (2021) Enhanced mechanical properties of 6082 aluminum alloy via SiC addition combined with squeeze casting. J Mater Sci Technol 88: 119-131.
5. Yuan D, Yang X, Wu S, Lü S, Hu K (2019) Development of high strength and toughness nano-SiCp/A356 composites with ultrasonic vibration and squeeze casting. J Mater Process Technol 269:1-9.
6. Britnell DJ, Neaileyand K (2003) Macrosegregation in thin walled castings produced via the direct squeeze casting process. J Mater Process Technol 138: 306-310.
7. Li R, Liu L, Zhang L, Sun J, Shi Y, Yu B (2017) Effect of squeeze casting on microstructure and mechanical properties of hypereutectic Al-xSi alloys. J Mater Sci Technol 33: 404-410.
8. Das P, Bhuniya B, Samanta SK, Dutta P (2019) Studies on die filling of A356 Al alloy and development of a steering knuckle component using rheo pressure die casting system. J Mater Process Technol 271: 293-311.
9. Li Y, Yang H, Xing Z (2017) Numerical simulation and process optimization of squeeze casting process of an automobile control arm. Int J Adv Manuf Technol 88: 941-947.
10. Wang Y, Xing S, Gao W, Wang T (2019) Research on a quantitative model of rheological distance by pressurizing. Mater Res Express 6: 0865b7.
11. Bai Y, Mao W, Gao S, TangG, Xu J (2008) Filling ability of semi-solid A356 aluminum alloy slurry in rheo-diecasting. Int J Miner, Metall Mater 15(1): 48-52.
12. Zhang H, Xing S, Zhang Q, Tan J, Liu W (2006) Evaluation of the mold-filling ability of alloy melt in squeeze casting. J Univ Sci Technol Beijing 13(1): 60-66.
13. Jahangiri A, Marashi SPH, Mohammadaliha M, Ashofte V (2017) The effect of pressure and pouring temperature on the porosity, microstructure, hardness and yield stress of AA2024 aluminum alloy during the squeeze casting process. J Mater Process Technol 245:1-6.
14. Lashkari O, Ghomashchi R (2007) The implication of rheology in semi-solid metal processes:

An overview. J Mater Process Technol 182: 229-240.
15. Mao W, Zheng Q, Zhu D (2010) Rheo-squeeze casting of semi-solid A356 aluminum alloy slurry. Trans Nonferrous Met Soc China 20: 1769-1773.
16. Wang H, Zhang YM, Zhou BC, Yang DH, Wu Y, Liu XJ, Lu ZP (2016) Mold-filling ability of aluminum alloy melt during the two-step foaming process. J Mater Sci Technol 32: 509-514
17. Wang Y, Xing S, Ao X, Wang T (2019) Microstructure evolution of A380 aluminum alloy during rheological process under applied pressure. China Foundry 16(6): 371-379.
18. Zeng J, Gu P, Zou Y, Xu Z (2009) Simulation of mold filling under counter gravity for A356 alloy and A356/SiCp composite. Mater Sci Eng A 499:130-133.
19. Li Y, Mao W, Zhu W, Yang B (2014) Rheological behavior of semi-solid 7075 aluminum alloy at steady state. China Foundry (11)2: 79-83.
20. Blanco A, Azpilgain Z, Lozares J, Kapranos P, Hurtado I (2010) Rheological characterization of A201 aluminum alloy. Trans Nonferrous Met Soc China 20(9):1638-1642.
21. Zoqui EJ, Paes M, Robert MH (2004) Effect of macrostructure and microstructure on the viscosity of the A356 alloy in the semi-solid state. J Mater Process Technol 153-154: 300-306.
22. Wang J, Shang S, Lu G, Yu J (2013) Viscosity estimation of semi-solid alloys based on thermal simulation compression tests. Int J Mater Res 104(3): 255-259.
23. Atkinson HV (2005) Modelling the semisolid processing of metallic alloys. Prog Mater Sci 50: 341-412.
24. Hu XG, Zhu Q, Lu HX, Zhang F, Li DQ, Midson SP (2015) Microstructural evolution and thixoformability of semi-solid aluminum 319s alloy during re-melting. J Alloys Compd 649: 204-210.
25. Ilkhchy AF, Jabbari M, Davami P (2012) Effect of pressure on heat transfer coefficient at the metal/mold interface of A356 aluminum alloy. *Int Commun Heat Mass Transfer* 39: 705-712.
26. Ma Z, Zhang H, Song W, Wu X, Jia L, Zhang H (2020) Pressure-driven mold filling model of aluminum alloy melt/semi-solid slurry based on rheological behavior. *J Mater Sci Technol* 39: 14-21.
27. Chattopadhyay H (2007) Simulation of transport processes in squeeze casting. *J Mater Process Technol* 186:174-178.
28. Hu XG, Zhu Q, Atkinson, Lu HX, Zhang F, Dong HB, Kang YL (2017) A time-dependent power law viscosity model and its application in modelling semi-solid die casting of 319s alloy. *Acta Mater* 124: 410-420.
29. Ma Z, Zhang H, Zhang X, Wu X, Fu H, Jia L, Zhang H (2019) Rheological behaviour of partially solidified A356 alloy: Experimental study and constitutive modelling. *J Alloys Compd* 803: 1141-1154.
30. Chang QM, Chen CJ, Zhang SC, Schwam D, Wallace JF (2021) Effects of process parameters on quality of squeeze casting A356 alloy. *Int J Cast Met Res* 23(1): 30-36.
31. Goh CS, Soh KS, Oon PH, Chua BW (2010) Effect of squeeze casting parameters on the mechanical properties of AZ91-Ca Mg alloys. *Mater Des* 31:S50-S53.
32. Gurusamy P, Prabu SB (2013) Effect of the squeeze pressure on the mechanical properties of the squeeze cast Al/SiCp Metal Matrix Composite. *Int J Microstruct Mater Prop* 8(4/5): 299-312.
33. Skolianos SM, Kiourtsidis G, Xatzifotiou T (1997) Effect of applied pressure on the microstructure and mechanical properties of squeeze-cast aluminum AA6061 alloy *Mater Sci*

Eng A 231:17-24.